Data-Driven Methodology for the Investigation of Riding Dynamics: A Motorcycle Case Study

Mirco Bartolozzi, Abderrahmane Boubezoul, Samir Bouaziz, Giovanni Savino, Stéphane Espie

Data-Driven Methodology for the Investigation of Riding Dynamics: A Motorcycle Case Study

Mirco Bartolozzi, Abderrahmane Boubezoul, Samir Bouaziz, Giovanni Savino, and Stéphane Espié

***Abstract*— Powered-Two-Wheelers (PTW) riders' fatalities are prevalent on bends outside built-up areas due to the complexity and instability of their vehicles: countermeasures require a better understanding of the rider-PTW interaction. Analysing riding data is effective but becomes challenging when using extensive datasets; segmenting the riding data would help identify events of interest, isolate specific manoeuvres and describe the riding session. Manual segmentation would be time-consuming and subjective; automation would be beneficial. This work proposed an automatic, unsupervised tool for segmenting and clustering signals acquired during a riding session for studying motorcycle lateral dynamics in-depth. The method only requires measuring the motorcycle roll angle. An expert rider completed a closed route using an instrumented motorcycle; the algorithm divided the time series into segments categorised into clusters relative to specific riding conditions. Analysing the segmented trial revealed the effectiveness and usefulness of the approach. Then, a corner entry manoeuvre was investigated in-depth to observe each segment's properties. The method associated each riding primitive to a cluster and described each manoeuvre through the segments' succession. The clusters were unambiguous and easy to interpret thanks to their dynamics-based nature and minimal overlap. The algorithm identified the differences between the three corner entry manoeuvres in the trial. The segmentation simplified the in-depth corner entry analysis and allowed early detection of the manoeuvre start. The proposed tool can aid research on motorcycle dynamics, PTW-rider interaction, and riding preferences in bends. The segmented time series could be employed for rider training and pre-crash fall dynamics reconstruction.**

***Index Terms*— Powered two-wheelers, motorcycle lateral dynamics, unsupervised clustering and segmentation, time-series, bend negotiation.**

I. Introduction

POWERED Two Wheeler (PTW) riders face a greater likelihood of experiencing fatal or severe injuries compared to other road users. In 2019, the French Road Safety Observatory (ONISR) accident report indicated that the PTW user category had a notably high percentage of injuries (26%) and fatalities (23%) [1]. Similar situations have been observed in other countries, and the World Health Organization has reported that two- and three-wheeled vehicles are involved in the majority of road fatalities [2]. It is concerning to note that PTW users account for just 2% of road users in France. Despite this elevated risk, the market for PTWs has grown significantly in recent years. The positive shift towards public transportation in congested urban areas has reinforced this trend.

The ONISR has released data indicating that 49% of all PTW user fatalities outside built-up areas occur on bends. Loss of control on bends, including traffic roundabouts and intersections, is likely due to the complicated dynamics and instability of PTWs. When motorcycles lean on bends, the risk of skidding increases, especially on poorly maintained road surfaces. In order to develop effective measures to reduce the risk of fatalities, observing the interaction between riders and their motorcycles on bends is necessary. By understanding motorcyclists' behaviour, road design and operation can be improved, and new training measures can be developed. Traffic laws can also be modified, and rider assistance devices can be created to enhance the safety of PTW users. It is crucial to precisely understand riders' behaviour to build active safety systems that do not impact their balance. In addition, understanding the interaction between riders and their PTWs is crucial for creating motorcycle riding simulators that are widely accepted and do not cause simulator sickness.

To comprehend riding behaviour, Vlahogianni et al. [3] recommends monitoring, recording, and analysing it. By studying the collected data, riders' behaviours during the bend-taking process can be understood effectively. Precisely identifying the various manoeuvres executed, their commencement and termination points, and intermediate stages is necessary to analyse the dataset thoroughly. Subdividing the time signals in a succession of distinct phases is called *segmentation*: having a segmented dataset allows one to identify events of interest, describe the characteristics of the riding session, compare different runs based on the succession of their segments and their respective lengths, and in general it facilitates the work of the expert that is studying the data.

Doing so is particularly challenging when aiming to describe a specific manoeuvre or phenomenon in-depth. A small error in the time instant could miss the event considered. Datasets relative to naturalistic riding are troublesome, too, as the manoeuvres executed are unknown *a priori*.

Manuscript received 20 December 2022; revised 27 March 2023; accepted 25 April 2023. Date of publication 9 May 2023; date of current version 30 August 2023. This work was supported by the Agence Nationale de la Recherche (ANR), France, through the VIROLO++ Project under Grant ANR-15-CE22-0008. The Associate Editor for this article was S. P. Raja. *(Corresponding author: Mirco Bartolozzi.)*

Mirco Bartolozzi and Giovanni Savino are with the Department of Industrial Engineering, University of Florence, 50121 Florence, Italy (e-mail: mirco.bartolozzi@unifi.it).

Abderrahmane Boubezoul and Stephane Espie are with TS2/SATIE/MOSS, Université Gustave Eiffel, 77420 Champs-sur-Marne, France (e-mail: abderrahmane.boubezoul@univ-eiffel.fr).

Samir Bouaziz is with SATIE/MOSS, Université Paris-Saclay, ENS Paris-Saclay, CNRS, SATIE, 91190 Gif-sur-Yvette, France.

Digital Object Identifier 10.1109/TITS.2023.3271790

Moreover, the database is often extensive in this case, and manual labelling and interpretation would be costly and possibly unfeasible. For example, Tokey et al. studied the spatial and temporal dynamics of e-scooters in an urban area: the study focused on general user behaviour, as manually segmenting individual trips would not have been possible due to the high number of trials considered and the granularity of the riding data used [4]. These aspects make automatic dataset segmentation extremely valuable, as labelled and interpreted data can be used to compare and investigate specific features. More detailed data should aid in predicting individual mobility [5] and key performance indicators for ride pooling [6], and individual- and road-section-dependent riding risk [7].

An automatic segmentation and clustering method could be used to advance scientific research. For example, research on riding style would benefit from comparing different riders, both holistically (e.g. comparing segments length and order for the same path) and regarding specific phases of the manoeuvre of interest (e.g. detecting the manoeuvre start to analyse the earliest phase of corner entry, as was manually done in Diop et al. [8]). Doing this would also facilitate comparing different trials for the same rider to scrutinise average tendencies and behaviour variability when given the same or different instructions. It would also enable identifying the rider's skill level from naturalistic riding instead of less representative tests in a controlled environment. Concerning this, Will et al. [9] studied riding style through g-g diagrams of long naturalistic sessions. Similar studies would benefit from plotting this diagram limitedly to specific manoeuvres or some of their phases, and statistical conclusions could be derived. Other studies on human-machine interaction could benefit from this. For example, describing motorcycle manoeuvrability [10] for different manoeuvres would become possible after automatically identifying those of interest. Some parametric identification procedures, such as characterising a motorcycle tyre through riding data [11], would benefit from finding the manoeuvres needed in a naturalistic riding dataset.

Riding trainers, too, could use such a tool. They could employ it during training to assess the skill level evolution or during the license test to compare the candidate to some reference riders to evaluate them. It could also be used by race engineers to quickly detect anomalies during a lap or by insurance experts to reconstruct accidents from black box data.

Different statistical tools or procedures can be designed to select interesting patterns in the riding episode. Nowadays, the identification of these patterns is manually achieved by researchers reviewing the video footage and signal readings, too, if available. This method is time-consuming and ineffective in identifying patterns in an extensive database, such as those collected in naturalistic riding studies. The alternative is using some proposed methodologies based on machine-learning techniques. There are two learning frameworks: supervised learning, where the model requires labelled training data, and unsupervised learning, which does not need labels for the data. *Labels* are the different time ranges of each segment or event (start and end times) that an expert could determine.

One of the drawbacks of supervised machine learning methods is that labelling the data collected during an experiment, such as detecting critical riding situations, can be challenging. Researchers review the video footage recorded during the experiment to manually identify the start and end times of each critical situation encountered by the rider during their travels. This extraction task is time-consuming and tedious. Another issue related to this labelling phase is that manual labelling tasks can introduce label errors, particularly in the transition between different segments.

The methods based on unsupervised learning algorithms aim to mine the experimental data without preconceived ideas. Researchers designed and conducted experiments to test a certain number of hypotheses. For that purpose, the algorithm will segment the data and create classes of riding behaviours. The challenge is to give a physical meaning to these classes to analyse the observed behaviours. The main issue behind such approaches is converging toward the optimal number of classes to explain the behaviours of interest.

This article aims to develop an automatic, unsupervised tool for the in-depth study of motorcycle dynamics and human-machine interaction. The cost-effective and objective nature of the approach is evident; however, the following research questions must be answered concerning the application of the method to a single trial:

- Is the method general and robust enough to be applied to different manoeuvres?
- Are the obtained clusters relative to distinct dynamic conditions, and is it possible to easily and unambiguously interpret them?
- Are there clear benefits of using this clustering and segmentation algorithm when studying a manoeuvre in-depth, like a corner entry manoeuvre?
- Can the method differentiate between analogous manoeuvres, like corner entries with different dynamics?

The research questions were not investigated regarding transferability to different riders or trials of the same rider. In particular, the article focuses on lateral dynamics, particularly the lean angle and its derivatives, as the roll is descriptive of the grip requested, and its evolution may reveal instabilities.

A. Related Works

Several research studies have been devoted to detecting driving patterns using unsupervised methods to analyse driving behaviour and detect risky driving situations in the case of four-wheeled vehicles. Some approaches rely on segmenting the Inertial Measurement Unit (IMU) time-series data, then applying clustering to group the driving primitives into classes [12]. Another research work addresses this issue by proposing an approach based on a high-level understanding of the driving behaviour through decomposing the IMU data into linear segments and assigning each segment to a convex optimisation of high-level driving behaviours [13]. Recently, an unsupervised approach was described in [14]; the proposed methodology is based on a two-step framework. The first

step involves applying Bayesian multivariate linear regression models to segment driving sequences into fragments. The second step applied extended latent Dirichlet allocation models to cluster the fragments into multiple descriptive driving patterns.

The research mentioned above applied a two-step framework: segmentation and clustering steps separately. The main limitation of doing so is related to the fact that these proposed methodologies will not consider the sequential aspect of the vehicle driving process. As a consequence, such approaches will not detect fine-grained patterns well.

In the case of the PTWs, the literature on the detection of riding patterns using unsupervised methods is less abundant compared to four-wheeled vehicles and peculiarly in the study of the bend-taking manoeuvre. One can cite [15], where the authors decomposed cornering manoeuvres based on roll dynamics. The rider's control strategies were decoupled into two classes based on the type of manoeuvre primitive: stationary, and dynamic, to estimate a personal rider skill score while riding on a winding road. Moreover, recently, in [8], unsupervised learning methods were used for the global analysis of the trajectory of a PTW during bend-taking. The same authors in [16] focused on the curve entry analysis by developing an unsupervised framework. The first step of the proposed methodology consists in automatically segmenting riding sequences to detect the bend entry. Then an extract of statistical features from the first two segments constituting the bend entry was used as inputs of a classifier to classify the riding behaviours.

Due to the limited and very recent emergence of automatic segmentation methods for PTWs, studies on handling and manoeuvrability used manual segmentation to divide the manoeuvres into different phases. Cossalter and Sadauckas [10] manually segmented the lane change manoeuvre into five segments based on some signals of interest's relative minima and maxima. This approach is appropriate when dealing with limited repetitions of a specific manoeuvre. However, it would be unfeasible in the case of a broader database of more general manoeuvres due to its lack of generality.

The paper structure follows: Section II describes the trial, the measuring instruments and the corresponding signals along with the sign convention, the segmentation algorithm used, the input signals chosen, and the method used to interpret the obtained clusters. Section III presents the interpreted clusters and the segmentation results, first for the entire trial and then focusing on the corner entry manoeuvre. These results are discussed in Section IV; a particular focus is given to the possible transitions between clusters. Possible extensions of the methods are proposed and justified. Lastly, Section V summarises the findings and implications and considers this work's applications and the subjects that might be interested in it.

II. Methods

The methodology, described in this section in more detail, was the following:

1) An expert rider completed a route closed to traffic on an instrumented motorcycle, producing a dataset of various time series.
2) A set of suitable signals linked to the lateral dynamics was chosen as the basis for the segmentation. The unsupervised segmentation algorithm used this set to segment the time series and categorised them into a chosen number of clusters.
3) The clusters were interpreted, each associated with a specific state linked to the lateral dynamics.
4) The entire segmented trial was analysed to evaluate the approach's usefulness and derive conclusions on its generality.
5) An in-depth analysis was conducted on a specific corner entry manoeuvre to observe the properties of each segment in more detail.

A. Trial Description

The data used in this paper come from a cornering experiment using a heavily instrumented motorcycle on the La Ferte Gaucher track [8]. The experiment aimed to understand how motorcyclists enter a turn, control their path, and exit using a group of experienced and novice riders. In this paper, The data of a single trial by a professional trainer of military riding trainers is used: a 40-year-old man with 19-year-old riding experience. This choice is based on such a rider's high experience and consciousness. Comparing qualitatively the signals acquired from three consecutive trials of that rider, significant repeatability in the riding behaviour emerged.

B. Measuring Instruments

The instrumented motorcycle was shown and described in detail in Diop et al. [8], which was relative to a different test campaign. Only a subset of those measuring instruments was used for this article:

- An MTi Xsens IMU provided the accelerations and Euler angles along the three axes.
- The standard Hall-effect sensor on the rear wheel measured the longitudinal speed.
- A magnetic sensor (AS5047P by AMS) acquired the handlebar steering angle.
- Four strain gauges on each handlebar acquired the longitudinal and vertical force acting on it. These forces were used to compute the resulting steering torque acting on the handlebar, considering the inclination of the steering axis.
- Another IMU (Tea Ergo CAPTIV Motion) was placed on the top of the helmet to acquire the orientation of the rider's head.

C. Signals and Sign Convention

Fig. 1 shows the sign convention used: the x-axis pointed forwards, the z-axis upward, and consequently, the y-axis leftward. Therefore, the roll angle ϕ was positive when the motorcycle was tilted to the right. A positive yaw angle ψ indicated an anti-clockwise rotation when the motorcycle is seen from above. The *head relative yaw angle* $\Delta\psi_{\text{head}}$

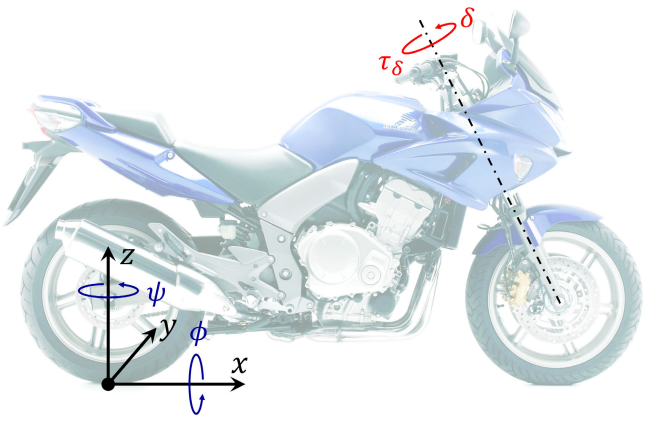

Fig. 1. The coordinate system used in this study, showing the positive directions for roll ϕ and yaw ψ motions. The positive direction for the steering angle δ and the steering torque τ_δ is also shown.

TABLE I
NOTATION OF THE SIGNALS AND THEIR UNITS

Notation	Description	Unit
ϕ	Roll Angle	$^\circ$
$\dot{\phi}$	Roll Rate	$^\circ\,\mathrm{s}^{-1}$
$\ddot{\phi}$	Roll Acceleration	$^\circ\,\mathrm{s}^{-2}$
$\dot{\psi}$	Yaw Rate	$^\circ\,\mathrm{s}^{-1}$
v	Longitudinal Velocity	$\mathrm{m\,s}^{-1}$
a_x	Longitudinal Acceleration	$\mathrm{m\,s}^{-1}$
δ	Steering Angle	$^\circ$
τ_δ	Steering Torque	$\mathrm{N\,m}$
$\Delta\psi_{\text{head}}$	Head Relative Yaw Angle	$^\circ$

was defined as the angle between the rider's head and the motorcycle symmetry plane: $\Delta\psi_{\text{head}} = \psi_{\text{head}} - \psi_{\text{bike}}$. It was positive when the rider looked at the bike's left. The reference frame was non-tilting: the x and y axes belonged to the ground plane, independent of the pitch and roll angles. The steering torque τ_δ and steering angle δ were defined around the steering axis. Both were positive if pointing upwards. For most motorcycles and riding conditions, the steering torque that the rider must apply to manoeuvre has a sign opposite to the yaw rate. When the yaw rate is positive (anti-clockwise, leftward corner), the steering torque is generally negative (clockwise): this phenomenon is referred to as *counter-steering*. Counter-steering can also refer to the steering angle during brief instants on corner entry. In this case, in the previous example, the steering angle would initially become negative (clockwise) as the steering torque. The signals used in this work are summarised in Table I.

D. Unsupervised Segmentation Algorithm

Toeplitz Inverse Covariance-Based Clustering (TICC) [17] is a model-based clustering technique that identifies repeated patterns in time series data by segmenting it into a fixed number of states, **K**. These states are represented by clusters and are characterised by a correlation network called a Markov Random Field (MRF). The MRF describes the relationships between the different variables within a state over a window of size w. The algorithm learns each cluster's MRF by estimating a sparse Gaussian inverse covariance (Toeplitz) matrix. Previous research by the authors [18] has shown that TICC outperforms other clustering methods like Hidden Markov Model and Gaussian Mixture Model in identifying riding patterns on simulator data. Each of the three metrics considered ('Silhouette', 'Calinski-Harabas', and 'Davies-Bouldin') showed a clear outperformance of the TICC algorithm.

The TICC approach utilises multivariate time series data as its input, represented by $\boldsymbol{x} = [\boldsymbol{x}_1, \ldots, \boldsymbol{x}_T]$, where T is the number of observations and $\boldsymbol{x}_i \in \mathbf{R}^n$, with n denoting the number of input signals. Clustering is conducted on short sequences of size $w \ll T$, with the newly generated sequences designated as $\mathbf{X}$=$\{X_1,\ldots,X_T\}$.

For the purposes of this discussion, $\mathcal{P} = \{P_1, \ldots, P_k\}$ represents the point assignments and $\Theta = \{\Theta_1, \ldots, \Theta_K\}$ denotes the Toeplitz matrices, where $\Theta_i \in \mathbf{R}^{nw\times nw}$. The optimisation problem can be formulated as follows:

$$\underset{\boldsymbol{\theta}\in\mathcal{T},\boldsymbol{P}}{\operatorname{argmin}} \sum_{j=1}^{k} [\overbrace{\|\lambda \circ \Theta_j\|_1}^{\text{sparsity}} + \sum_{Y_i\in P_j} (\overbrace{\ell\ell\left(Y_i,\Theta_j\right)}^{\text{log-likelihood}} + \overbrace{\beta\mathbf{1}\{Y_{i-1}\notin P_j\}}^{\text{temporal consistency}})] \quad (1)$$

The TICC algorithm incorporates two key regularisation parameters, λ and β. The first parameter, λ, governs each cluster's sparsity of the Markov Random Field (MRF) matrices. It shares the same shape as the MRFs ($\lambda \in \mathbf{R}^{nw\times nw}$), but for practical reasons, λ can be reduced to a single value to streamline the search process. The second parameter, β, is responsible for enforcing temporal consistency and continuity between adjacent subsequences. It imposes a penalty for smoothness, and a higher value of β promotes the grouping of neighbouring subsequences into the same cluster.

TICC incorporates two additional parameters:

- **Window size (w)**, which specifies the number of observations within a given subsequence, represented by $X_t = [x_{t-w+1}, \ldots, x_t]$, with $X_t \in \mathbf{R}^{n\times w}$. All observations within the same subsequence are grouped together and assigned to the same cluster.
- **Number of clusters (K)** corresponds to the number of patterns that need to be identified. This value can be determined using either the BIC or silhouette score, but its selection is typically dependent on the application.

The optimisation problem is solved by initially randomising the Toeplitz matrices, Θ, and cluster assignments, **P**, and then utilising a variation of the expectation maximisation (EM) algorithm, which alternates between assigning subsequences (update **P**) and updating the clusters' parameters (Toeplitz matrices), Θ.

E. Input Signals

The segmentation aimed to identify the different cornering phases using a limited set of easily measurable signals. The roll angle ϕ was chosen as one of the input signals for the algorithm, as it is the primary state related to the lateral dynamics. It allowed differentiating between low, medium and high roll angle riding. However, the actual riding condition was also defined by how fast the roll angle changes: a $\phi \approx 0$ condition could be either a straight riding condition or the

intermediate, brief section of a change of direction. Therefore, the roll rate $\dot{\phi}$ was added. Even though these two signals could identify diverse riding conditions, some short sections with particular characteristics would have been lumped with others. Consider a corner entry manoeuvre: the algorithm would differentiate between straight riding (low roll) and tilting fast (high roll rate). The roll rate, however, was not generated instantly: it would reach high values when the roll was already significantly higher than zero. The intermediate segment would be partially lumped with the previous straight-riding segment and, for the remaining part, with the following fast-leaning segment. The roll acceleration $\ddot{\phi}$ was also considered to detect the manoeuvre start sooner and give more depth to the analysis. The advantage of using these three signals was that the roll rate and roll acceleration are the derivatives of the roll angle. Therefore, the approach allowed an in-depth description of the lateral dynamics starting from a single signal (the roll angle).

Using the roll angle directly would produce two different clusters for the right ($\phi > 0$) and left ($\phi < 0$) corners. As the corner direction does not influence the symmetrical rider-motorcycle system's behaviour, the roll angle's absolute value $|\phi|$ was used. Similarly, the roll rate sign tells about the direction (left or right) of the lean velocity; instead, knowing whether the roll rate increased or decreased the roll angle was more interesting. The new signal $\dot{\phi}' = \dot{\phi}\,\mathrm{sign}\,\phi$ was defined: when the roll angle and roll rate had the same sign, the roll increased in absolute value, and $\dot{\phi}' > 0$. The opposite held for $\dot{\phi}' < 0$. Similarly, a new variable was defined concerning the roll acceleration: $\ddot{\phi}' = \ddot{\phi}\,\mathrm{sign}\,\phi$. To summarise, the segmentation algorithm used the following signals:

$$|\phi|\,, \quad \dot{\phi}' = \dot{\phi}\,\mathrm{sign}\,\phi, \quad \ddot{\phi}' = \ddot{\phi}\,\mathrm{sign}\,\phi. \tag{2}$$

The algorithm based the segmentation only on these signals. The segments identified were the same for all the signals. The TICC parameters chosen were: $\lambda = 5 \times 10^{-4}$, $\beta = 5$, $w = 1$ and $K = 6$.

F. Clusters Interpretation Method

The algorithm was unsupervised; therefore, the obtained clusters had to be interpreted. To this end, the input signals were plotted in pairs using a scatter plot. A specific colour represented the data points relative to the same cluster. The typical input signals values corresponding to each cluster were derived by looking at the position of its points. Representing the dispersion along each variable through box plots aided this process. Each cluster was linked to the manoeuvre type or its specific phase through the theory of motorcycle dynamics.

III. Results

A. Interpreted Clusters

The three variables used as input to the algorithm ($|\phi|$, $\dot{\phi}'$, $\ddot{\phi}'$) were plotted against each other in pairs (Fig. 2) to interpret the six different clusters.

Fig. 2a plots $\dot{\phi}'$ against $|\phi|$. Two clusters (blue and orange) had a zero-median roll rate: the former included data points with minimal roll, while the latter had a very high roll.

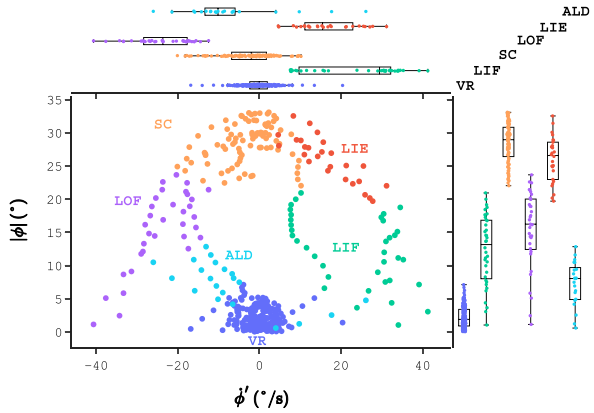

(a)

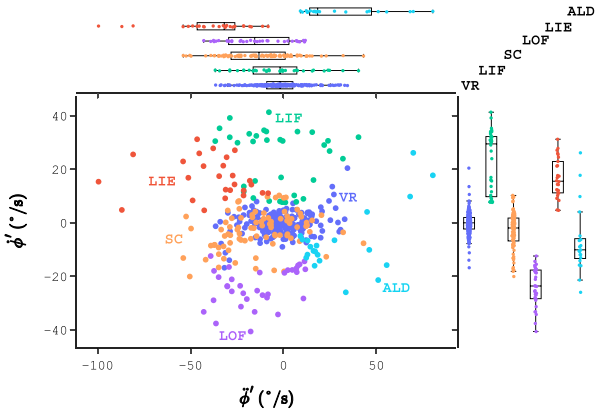

(b)

Fig. 2. Scatter plots of the input signals for the segmentation algorithm, represented in pairs, showing the different clusters for the trial. (a): Roll angle absolute value and roll rate in lean direction. (b): Roll rate in lean direction and roll acceleration in lean direction. Clusters are: VR (Vertical Riding); SC (Steady Cornering); LIF (Lean-In Fast); LOF (Lean-Out Fast); LIE (Lean-In End); ALD (Accelerating in Lean Direction).

Therefore, the blue cluster was relative to the motorcycle being vertical, while the steady corners made up the orange one (Fig. 2b). $\ddot{\phi}'$ had a zero median for the blue cluster but a negative one for the orange cluster: given that $\ddot{\phi}' = \ddot{\phi}\,\mathrm{sign}\,\phi$, this means that, on average, during a corner, the roll acceleration produced a roll rate that tended to reduce the roll angle. In fact, the absolute value of the roll angle signal had a negative second derivative (the roll reached a peak, maintained it for the duration of the corner, and then reduced). Table II summarises the properties of each cluster: the blue cluster was named **'Vertical Riding' VR** and the orange one **'Steady Cornering ' SC** .

The green and purple clusters showed symmetrical behaviour: high $\dot{\phi}'$ values (positive and negative, respectively) and moderate roll values. Therefore, these clusters described rapid roll changes: towards higher ($\dot{\phi}' > 0$) and lower ($\dot{\phi}' < 0$) roll angle values, respectively. Therefore, the green cluster was named **'Lean-In Fast' LIF** and the purple one **'Lean-Out Fast' LOF** .

TABLE II
THE SIX CLUSTERS WITH THEIR ASSOCIATED COLOURS AND THE CORRESPONDING VALUES AND DIRECTIONS OF THE ROLL ANGLE AND ITS DERIVATIVES. 'IN' INDICATES 'TOWARDS THE LEAN DIRECTION' 'OUT' INDICATES 'AWAY FROM THE LEAN DIRECTION

	ϕ	$\dot{\phi}$	$\ddot{\phi}$
VR	≈ 0	≈ 0	≈ 0
SC	High	≈ 0	Low (Out)
LIF	Medium	High (In)	≈ 0
LOF	Medium	High (Out)	Medium (Out)
LIE	Medium-High	Medium-Low (In)	High (Out)
ALD	Low	≈ 0	Medium (In)

The red cluster comprised medium to high roll angle values, with positive, medium $\dot{\phi}'$ values and negative, very high $\ddot{\phi}'$ values: the motorcycle was increasing its roll angle ($\dot{\phi}' > 0$) at an ever-decreasing rate ($\ddot{\phi}' < 0$). The motorcyclist was stabilising the motorcycle to the steady-state cornering roll angle: this red cluster was named **Lean-In End** **LIE** . The cyan cluster regarded low roll angle values, negative and medium $\dot{\phi}'$ values and high, positive $\ddot{\phi}'$ values. The motorcycle roll accelerated towards the lean direction ($\ddot{\phi}' < 0$) around the zero roll condition. Consequently, the rider was either stabilising the motorcycle towards a straight riding condition (if $\dot{\phi}' < 0$, therefore decreasing its roll) or destabilising it to initiate the corner entry (if $\dot{\phi}' > 0$, therefore increasing its roll). This cyan cluster was named **'Accelerating in Lean Direction'** **ALD** .

To conclude, each cluster represented one specific lateral dynamics condition. Three couples of clusters could be identified, as each cluster had a dual: VR-SC, LIF-LOF, and LIE-ALD. The three couples were characterised by their roll angle, roll rate and roll acceleration, respectively.

B. Complete Trial

Fig. 3 showed the motorcycle trajectory during the trial, divided into segments with the colour indicating the corresponding cluster. The segments were 27 in total, with four or five per cluster. The segments corresponding to the straights belonged to the 'Vertical Riding' cluster, and there was a 'Steady Cornering' segment for each bend. A VR segment was linked to the following SC segment (corner entry section) through either a LIF, LIF→LIE or ALD→LIF→LIE sequence. Conversely, an SC segment was always linked to the following VR segment (corner exit section) through a LOF→ALD sequence. In the case of the chicane, the two SC segments were always linked by a LOF→LIF→LIE sequence. The last segment belonged to the VR cluster, despite the slightly curved trajectory: the low speed ($v < 6\,\mathrm{m\,s^{-1}}$) produced a minimal roll angle, analogous to that experienced on a straight section.

Fig. 4 shows some relevant time series. In particular, Fig. 4a depicts the roll angle and its derivatives, from which the input signals of the segmentation algorithm were derived. This plot shows an alternative view compared to Fig. 2. The VR segments were characterised by roll angle values around zero; on the contrary, the SC segments stood out for their very high roll values, reaching 33.1 deg. The LIF and LOF

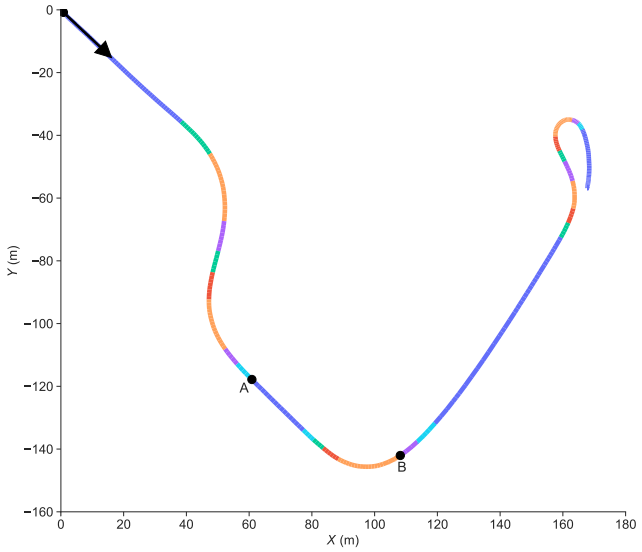

Fig. 3. Trajectory of the trial divided into segments. The colour of each segment indicates the cluster it belongs to: VR (Vertical Riding); SC (Steady Cornering); LIF (Lean-In Fast); LOF (Lean-Out Fast); LIE (Lean-In End); ALD (Accelerating in Lean Direction). The arrow indicates the direction of travel. Letters A and B delimit the corner entry manoeuvre analysed.

segments shared high roll rate values (maximum 41.3 deg/s). Still, while the former had a sign concordant with the roll angle (lean increasing), the opposite was true for the latter (lean decreasing). Lastly, the LIE and ALD segments showed the highest roll accelerations, reaching a maximum of 99.5 deg/s^2.

Fig. 4b shows additional signals. The longitudinal speed v and acceleration a_x described the longitudinal dynamics, which had not been not explicitly considered in the segmentation algorithm. For most of the trial, the speed was in the 5 m s^{-1} to 15 m s^{-1} range. The highest positive (4.3 m s^{-2}) and negative (-4.7 m s^{-2}) longitudinal acceleration values were achieved in the VR segments. The rider reduced the throttle and braking inputs in the other segments, where there was also a demand for lateral grip. The steering angle δ was around zero in the VR segments, except for the first instants (when the motorcycle was starting from a standstill) and the slow last segment. Its value was maximum in the SC segments, especially in the last one. Lastly, the steering torque τ_δ had a trend similar to the steering angle but with the sign reversed due to its generally counter-steering nature.

Requiring longitudinal grip reduced the available lateral grip and *vice-versa*. Different riders can combine longitudinal and lateral dynamics differently, originating g-g diagrams with different shapes [9]. Fig. 5 shows that, in this case, the g-g diagram had the 'Leaf' shape, typical of more aggressive riders [9]. The rider used the combined dynamics extensively, as indicated by the points often far from both axes. He tended to brake intensely with the motorcycle both vertical and tilted. In comparison, the reduction in the throttle request when the motorcycle was leaned was more evident, although he reached $\sim$ 2 m s^{-2} of positive longitudinal acceleration concurrently with high lateral acceleration values. While the maximum (positive or negative) longitudinal acceleration was achieved when the lateral acceleration was tiny, the

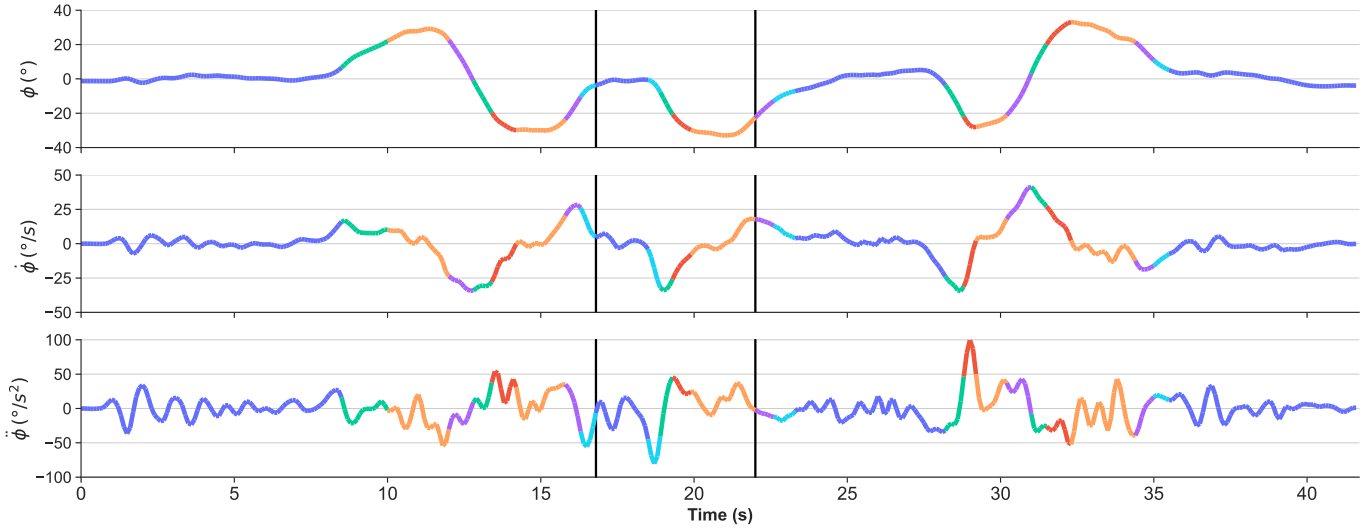

(a)

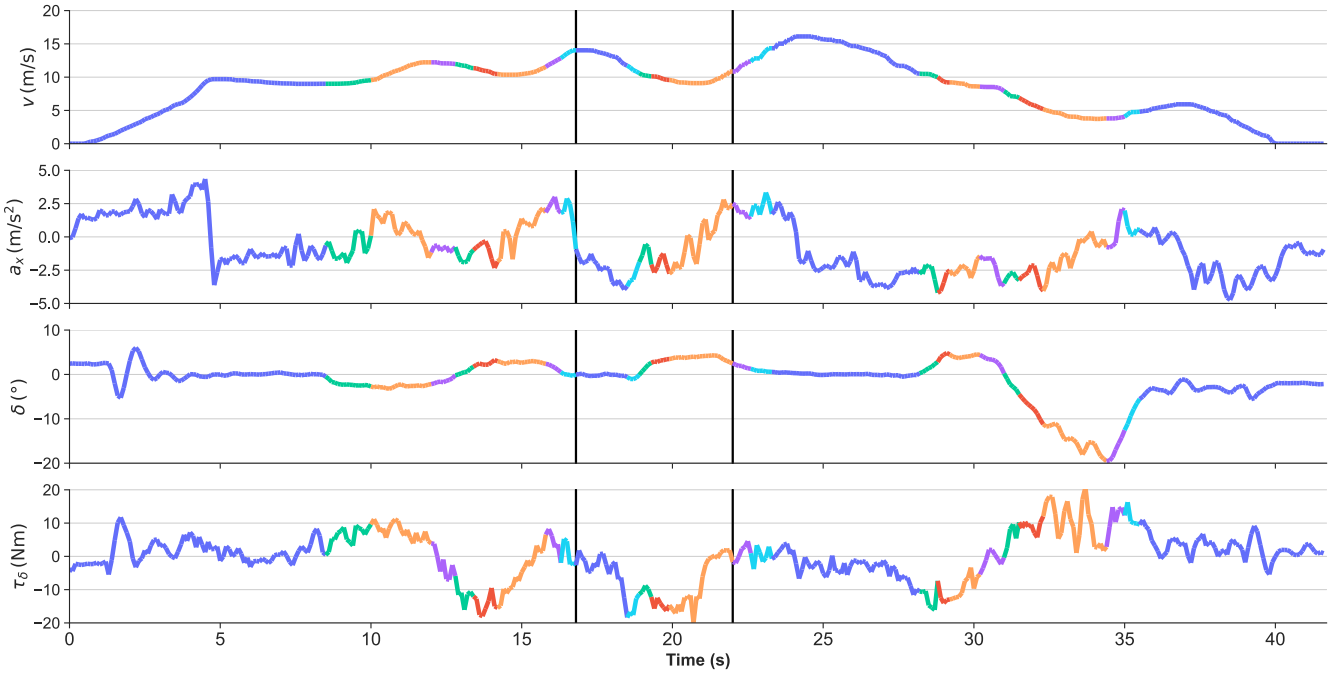

(b)

Fig. 4. Time series of relevant signals acquired during the trial. The colour of each segment indicates the cluster to which it belongs. The vertical lines indicate the beginning and the end of the corner entry manoeuvre analysed in depth. (a): Signals linked to those used in the segmentation algorithm (roll angle ϕ, roll rate $\dot{\phi}$, roll acceleration $\ddot{\phi}$). (b): Additional signals (speed v, longitudinal acceleration a_x, steering angle δ, steering torque τ_δ).

maximum lateral acceleration corresponded to moderate decelerations. Therefore, the maximum roll was reached before the motorcycle speed had reached its minimum. The LIE cluster had a negative median longitudinal acceleration and was strictly within the lower half of the graph: the rider never used the throttle right before reaching the maximum roll. This fact is primarily true also for the LIF cluster, which immediately precedes the LIE segments. Compared to the SC cluster, the points belonging to the LIE cluster had more negative longitudinal acceleration and lower lateral acceleration: the rider tilted the motorcycle less but braked more. The VR cluster had a negative median: the rider used the brake more than the throttle when the motorcycle was vertical.

C. Corner Entry Manoeuvre

Fig. 6 shows the corner entry manoeuvre analysed. In particular, Fig. 6a shows the time series of the roll angle and its derivatives, along with other significant signals (the steering angle δ, the steering torque τ_δ, the longitudinal acceleration a_x, and the head relative yaw angle $\Delta\psi_{\text{head}}$). The algorithm divided the manoeuvre into five segments: in order, VR (Vertical Riding), ALD (Accelerating in Lean

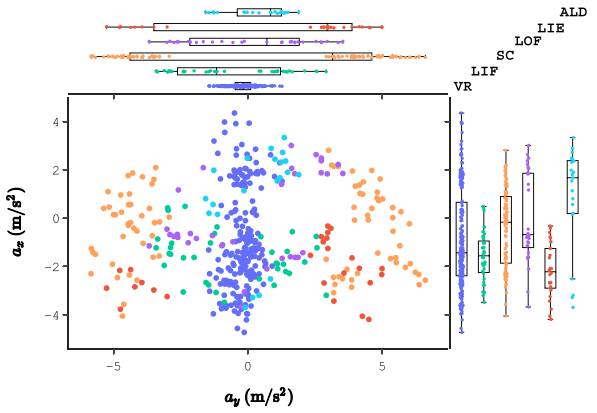

Fig. 5. g-g diagram, showing the different clusters for the trial. Clusters are: VR (Vertical Riding); SC (Steady Cornering); LIF (Lean-In Fast); LOF (Lean-Out Fast); LIE (Lean-In End); ALD (Accelerating in Lean Direction).

Direction), LIF (Lean-In Fast), LIE (Lean-In End), and SC (Steady Cornering). As shown in Fig. 6b, during this time, the motorcycle went from straight riding to cornering slightly after the corner apex. The behaviour in each segment is now described:

- VR . Initially, all signals related to the lateral dynamics fluctuated around zero; the longitudinal acceleration was small and negative (the rider was slowly reducing his speed), and the head relative yaw angle was around $+10°$ (looking slightly to the left, in the corner direction). Through the segment, the deceleration progressively increased up to its manoeuvre maximum. Towards the end of the segment, various signals moved from zero, indicating the initiation of the corner entry manoeuvre. The motorcycle is a causal system in that its response cannot anticipate the inputs: as the steering torque is the primary control input for the rider, it can be employed to detect the manoeuvre initiation instant. As the steering torque was negative throughout the following part, the last zero-crossing of the steering torque (dash-dotted circle in the figure) was considered as the 'corner initiation' instant. The negative sign indicated a clockwise steering torque, therefore counter-steering, the curve being anti-clockwise. This torque produced a tiny, negative (counter-steering) steering angle: the front wheel became misaligned with respect to the motorcycle velocity, generating a slip angle on the front tyre that produced a centripetal force. This force generated a moment around the centre of gravity of the motorcycle-rider system, resulting in a negative, leftward roll acceleration. Over time, this produced a roll rate barely measurable at the end of the segment. There was not enough time to vary the roll angle, as it is the second integral of the roll acceleration. The steering torque continued to increase, reaching 20 N m, which was close to the manoeuvre maximum.
- ALD . The steering torque remained high: the roll angle, which is generally responsible for a significant part of the reaction torques [19], was still tiny, but the roll rate was significant, so the applied torque had to compensate for the roll-related gyroscopic torque. The counter-steering torque applied by the rider exceeded the reactive torques, producing an increase in the steering angle, which was already counter-steering and reached a local maximum. This steering angle variation made the motorcycle yaw towards the outside of the corner (negative, rightward yaw rate). The video (Fig. 6a) confirmed this phenomenon. Towards the end of the segment, the roll angle and roll rate became significant: this increased the reactive torques, which the decreased applied torque could not overcome. The steering angle and, consequently, the yaw rate went towards zero while the roll rate reached its maximum. As the vehicle turned slightly towards the outside, the rider had to compensate by looking progressively more to the motorcycle's left (Fig. 6b).
- LIF . The roll rate reached its maximum value. The roll acceleration initially had a sign concordant with the roll rate (the motorcycle leaned faster and faster) and a discordant sign in the second part of the segment (the rider started to reduce the roll rate). In this segment, the steering angle and yaw rate became positive (towards the corner inside). This behaviour would continue for the remainder of the manoeuvre. The rider's head reached the maximum yaw angle relative to the motorcycle, around 27°.
- LIE . The segment linked the transient corner entry phase to the steady-state cornering phase identified by the last segment. The roll acceleration was discordant with the roll rate: the roll angle approached its maximum value at a decreasing rate. The motorcycle was reaching its new equilibrium (cornering): the signals linked to each other in a steady state (roll angle, yaw rate, steering angle and torque) showed the same dynamics, converging to their maximum value. The rider applied approximately constant steering torque and continued looking toward the corner inside.
- SC . The rider applied an approximately constant torque, reaching a new equilibrium: the roll, steering angle and yaw rate signals became constant, as did the head relative yaw angle. After reaching the apex, the rider prepared for the following straight: he reduced the steering torque (dashed circle) and started to align the head to the travelling direction. The steering torque went to zero in around 1 s, inducing a positive (rightward) roll acceleration responsible for the straightening phase. The roll angle, yaw rate and steering angle reduced in amplitude, which remained significant at the end of the segment.

The longitudinal acceleration was the only signal, among the previous ones, describing the longitudinal dynamics, which was not explicitly considered by the segmentation algorithm. The rider braked progressively more when closer to the corner apex: this strategy reduced the manoeuvre time for a given maximum acceleration and jerk and a specific speed decrease target. Then, as soon as the cornering started (second segment), the rider started reducing the braking action: the consequent

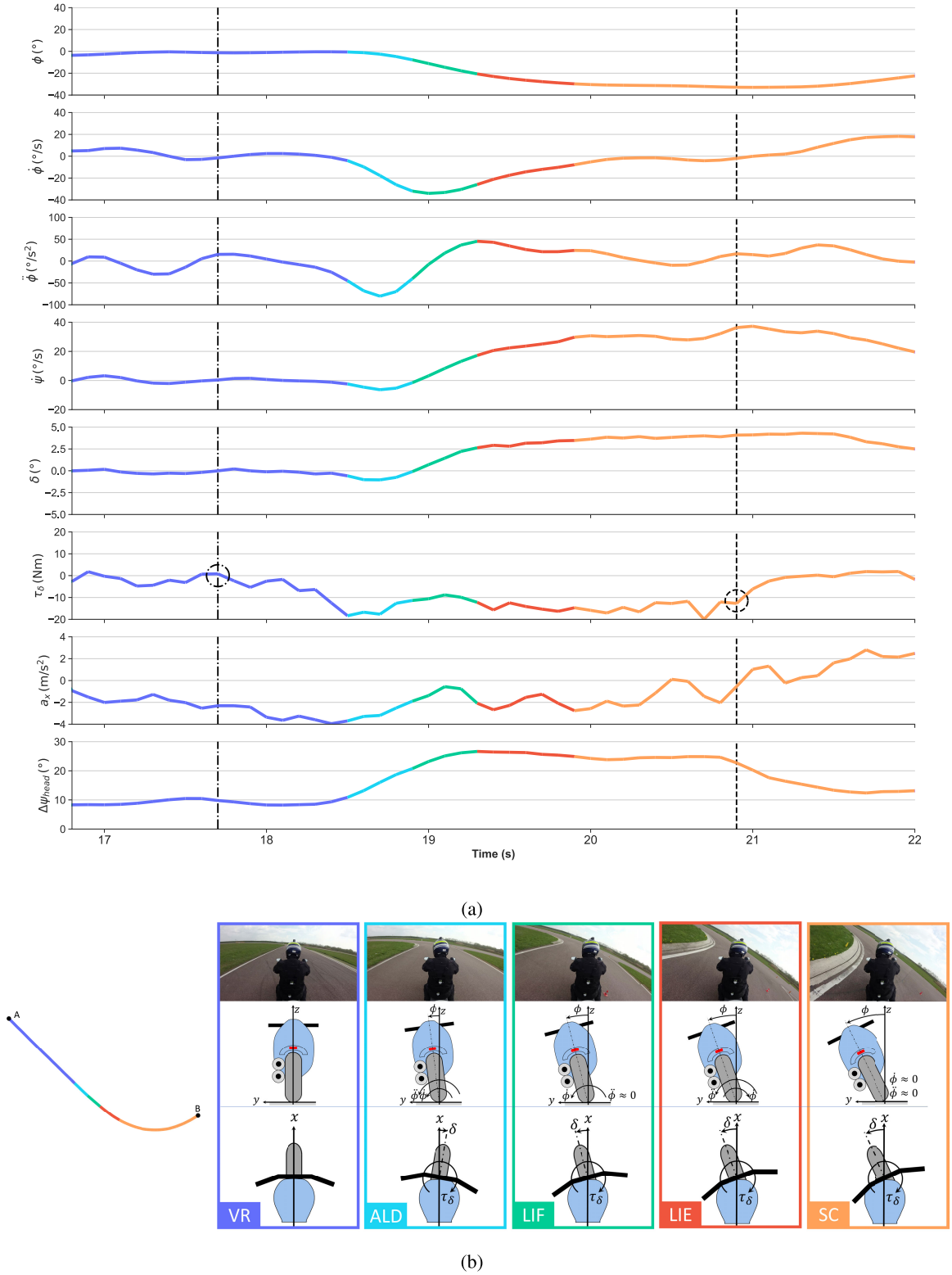

Fig. 6. Corner entry manoeuvre analysis. (a) Time series of relevant signals, comprising those linked to the signals used in the segmentation algorithm (roll angle ϕ, roll rate $\dot{\phi}$, roll acceleration $\ddot{\phi}$) together with additional ones (yaw rate $\dot{\psi}$, steering angle δ, steering torque τ_δ, longitudinal acceleration a_x, head relative yaw angle $\Delta\psi_{\text{head}}$). (b) Segmented trajectory (left) and properties of each segment (right). The frames at the top show the motorcycle heading and roll and the yaw of the motorcyclist's head. The drawings at the centre (rear view) describe the sign of the roll angle and its derivatives. The drawings at the bottom (top view) describe the sign of the steering angle and steering torque.

reduction of the requested longitudinal adherence increased the lateral grip. This strategy kept a relatively constant safety margin to the friction envelope. The longitudinal acceleration reached zero in the last segment (when the roll angle was maximum) and became positive (throttle input) when the roll started decreasing. The leftward 10° initial head relative yaw

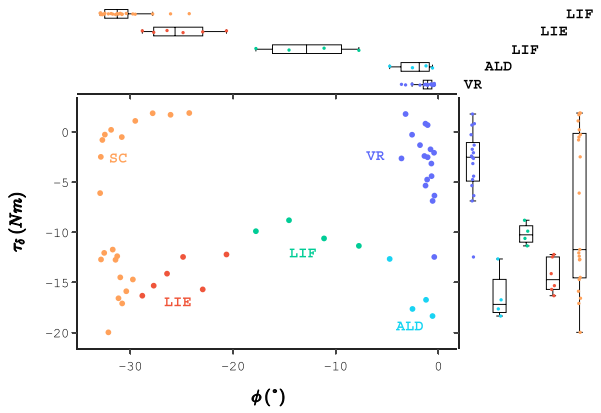

Fig. 7. Scatter plot of the steering torque, showing the different clusters for the corner entry manoeuvre.

angle was justified by the corner being preceded by another leftward corner: the rider did not completely straighten his head before aiming at the next bend. Fig. 4b showed that the steering angle had a similar (and opposite in sign) trend to the steering torque and tended to lag behind it. This fact is shown more clearly by Fig. 6a: the segments showed that, while the steering torque peak was at the end of the first segment (VR), that of the steering angle was in the following ALD segment. The steering torque remained counter-steering throughout the manoeuvre; the steering angle, instead, started to point towards the inside of the corner at the beginning of the third segment (LIF). The steering inertia acted as a low-pass filter from the torque input to the angle output: consequently, the former was more erratic than the latter.

Manoeuvrability is the response of a motorcycle to the rider's input: the effect of the control action becomes more apparent when the steering torque is shown against the resulting roll angle, as in Fig. 7. At the beginning of the manoeuvre (VR), the roll angle and the steering torque were null. The rider applied a sudden negative (clockwise) steering torque (dark blue point below the others): the roll did not have enough time to vary and remained around zero. The ALD segment began: the roll angle turned negative (leftward, therefore, the steering torque was counter-steering) while the rider continued to apply a significant steering torque. ϕ =5° marked the transition to the LIF segment: the rider lowered the applied torque slightly, as the roll angle allowed the motorcycle to lean itself (due to the moment arm of the weight force). The motorcycle tilted quickly, leading to the LIE segment: the rider increased the steering torque again and maintained it to reach the desired roll angle (SC segment). During the corner, the points were located in the lower-left corner (negative, leftward roll angle and negative, clockwise steering torque, therefore counter-steering). Towards the corner end, the rider reduced the applied steering torque to zero: this sudden variation did not induce an analogous roll reduction, as the process takes time to produce tangible effects. During a left corner, the rider must apply a clockwise torque to equal the resulting external, anti-clockwise torque. As soon as the applied steering torque reduced, this resultant turned the steering anti-clockwise: this rotation produced a tyre

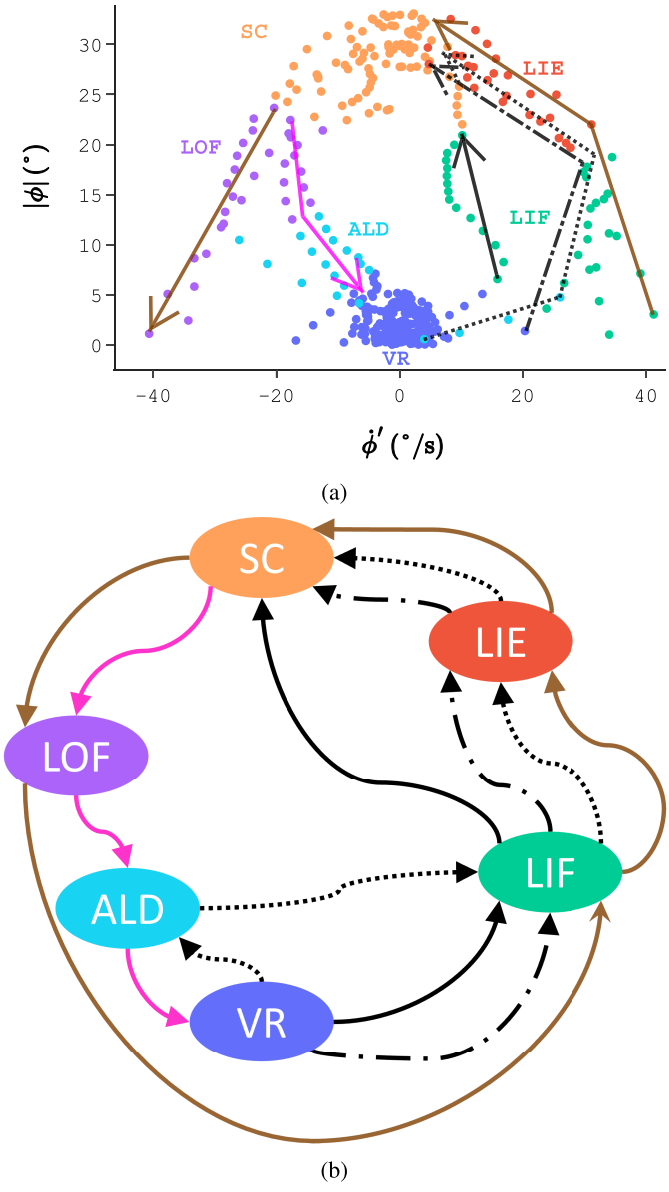

Fig. 8. Transitions between equilibrium states ('Vertical Riding' and 'Steady Cornering' clusters). The possible VR to SC transitions (corner entry) are indicated in black, the SC to VR transition (corner exit) is in pink, and the SC to SC transition (chicane) is in brown. (a): Scatter plot of the roll angle absolute value and roll rate in the lean direction. (b): Conceptual scheme of the transitions.

lateral force in the centripetal direction that automatically straightened the bike. In this case, the rider applied a small positive torque to speed up the straightening process.

IV. Discussion

A. Transitions Between Clusters

The clustering results (Fig. 2) showed that, concerning lateral dynamics, riding a motorcycle consists of frequent transitions between two states of equilibrium: 'Vertical Riding' (VR) and 'Steady Cornering' (SC). By definition, both are relative to zero roll rate and roll acceleration but are distinguished by their very different roll angle values. Fig. 8 shows the five transitions that occurred.

When approaching a corner, the rider went from VR to SC to VR, following an anti-clockwise[1] circle in the $(|\phi|, \dot{\phi}')$ diagram. However, the transition from VR to SC happened in three distinct ways:

- VR→LIF→SC (black, solid arrow). It was the case of the first corner (Fig. 3). The large corner radius allowed a gentle entry: the roll rate remained moderate (Fig. 4a), and the roll acceleration was very low, preventing the presence of'Accelerating in Lean Direction' (ALD) or 'Lean-In end' (LIE) segments.
- VR→LIF→LIE→SC (black, dash-dotted arrow). It was the case in the fourth corner. Similarly to the previous case, the initial part of the corner entry was very gradual, with a modest $\ddot{\phi}$ value, so the VR and LIF segments were not separated by an ALD segment. However, the final corner entry phase was more abrupt: the roll acceleration reached high values, introducing a LIE segment before the SC.
- VR→ALD→LIF→LIE→SC (black, dashed arrow). It was the case in the third corner. The first and last phases of the corner entry were both quick, producing significant roll acceleration values: these were characteristic of the ALD and LIE segments, which appeared around the LIF segment.

The difference in roll rate and roll acceleration values that produced the VR→LIF→SC or the VR→ALD→LIF→LIE→SC corner entry sequence was clear from Fig. 4a, comparing the entry in the first (8-12 s) and third (18-21 s) corners. For the latter, the maximum roll was slightly higher and was reached in a shorter time: this increased the frequency of the roll signal, increasing the roll rate and, even more so, the roll acceleration, which are proportional to the frequency and the frequency squared, respectively.

When going from cornering to straight riding, the transition was SC→LOF→ALD→VR (pink, solid line) in all three cases. This happened because the initial phase was always gradual, with modest roll acceleration, probably a rider safety choice considering the high initial roll angles. This graduality caused a direct SC→LOF transition, followed by an ALD segment, indicating that the final part of the manoeuvre was more abrupt than the beginning.

While an SC segment, among others, always connected two VR segments, the opposite did not hold: it was possible to move from one SC state to another without passing through a VR segment. This case was seen in the section between the first two corners: the transition was SC→LOF→LIF→LIE→SC (brown, solid arrows).

Fig. 8a shows all the transition paths between the two equilibrium states (VR and SC). The chicane was particularly interesting: a negative $\dot{\phi}'$ was generated, which reduced the initially high roll angle. However, the state continued towards the lower left corner instead of converging to the origin (VR). When $|\phi|$ reached zero, ϕ changed sign, and so did $\dot{\phi}'$: the points emerged from the lower right corner and converged towards SC, explaining the SC→LOF→LIF→LIE→SC transition. Fig. 8b conceptualises these transitions: all those between two specific clusters were unidirectional, except for that between VR and ALD, which happened both ways. This result was coherent with what was found in Section III-A: the ALD cluster can either indicate a stabilising (ALD to VR) or destabilising action (VR to ALD), depending on the sign of the roll rate in lean direction $\dot{\phi}'$.

[1]As $\dot{\phi}' > 0$ indicated increasing roll and the opposite for $\dot{\phi}' < 0$.

B. Results Discussion

The results positively answered the research questions, which were investigated concerning a single run of a professional riding trainer without specifically investigating transferability to other rides or riders. The method proved robust in describing the dynamics of different manoeuvres, like the entry and exit of corners of different radii, speed and frequencies, a change of direction and the straight sections connecting them. The algorithm divided the lateral dynamics into elementary primitives, each corresponding to a cluster with peculiar statistics regarding the three input signals.

By plotting the input signals in pairs (Fig. 2), it was possible to associate each with a corresponding lateral dynamics state. There was negligible overlap in the $(\dot{\phi}', |\phi|)$ diagram (Fig. 2a), making the clusters distinct and easy to interpret. The higher overlap in the $(\dot{\phi}', \ddot{\phi}')$ due to the VR and SC clusters is justified by the theory: riding straight and in a steady corner are both steady-state conditions, so the two derivatives must go to zero in both cases. These aspects made the clusters unambiguous and easy to interpret.

The case study presented also showed the method's usefulness on two levels. At the trial level, it was possible to examine different manoeuvres by comparing the types and order of the segments that make up each. For the trial considered, each of the three corner entry manoeuvres comprised a different number of segments, from three to five, albeit the order of the segments present did not change, as expected. This result showed that, due to the different corner geometry and possibly rider choice, different corner entry manoeuvres could have different dynamics, as confirmed by the time signals (Fig. 4). Instead, the three corner exits followed the same pattern. This lower variability on corner exit compared to corner entry should be investigated further on a higher number of trials and for different riders. Detecting this pattern by looking at the non-segmented time signals would have been difficult, even for an expert conducting a manual segmentation or creating the reference for the supervised segmentation. The segmentation and clustering process made some aspects more evident. Fig. 2b showed that $\dot{\phi}'$ and $\ddot{\phi}'$ had a higher variance in the SC cluster compared to the VR one: keeping an approximately constant roll was harder when cornering than during straight riding, requiring more corrections that reflected on the variance. Even though this result was expected, the method made it straightforward to compare the variances of each signal in these two distinct riding conditions. The ALD segment is relative to high roll-acceleration values. As cornering with a high roll and producing a high roll acceleration are both demanding, the rider produced high roll accelerations only when the roll angle was small (Fig. 2a). Fig. 3 confirmed that this happened only

at the beginning or at the end of a Vertical Riding segment, where the rider was perturbing and stabilising the motorcycle, respectively.

On the manoeuvre level, the segmentation simplified the in-depth corner entry analysis. Each segment was relative to a distinct manoeuvre phase, as Fig. 6 showed through the time signals, the GPS trajectory and a video frame for each segment. The roll acceleration signal was included among the input signals mainly to detect the manoeuvre start early: the goal was achieved, as the corner entry was detected when the roll angle was still around 0.5°. In fact, in that instant, the roll acceleration was already $45\,^{\circ}\,s^{-2}$. This approach was chosen not to use the rider commands (as the steering torque) as inputs to the algorithm. Measuring the roll and its derivatives is particularly straightforward, making the method more general and easier to apply. Still, the manoeuvre start was promptly detected: Fig. 7 shows that the ALD segment started with the second data point of those having a steering torque significantly different from zero. Using the steering torque as input could make the detection almost instantaneous. Future work could also consider using solely rider inputs (throttle, brake, and steering torque) instead of the resulting motorcycle motion (the roll angle, its derivatives, and the longitudinal acceleration).

The input signals were all relative to lateral dynamics, so the longitudinal motion did not directly influence the results. Therefore, while the input signals fluctuated around zero in the VR segments (Fig. 4a), Fig. 4b showed that the speed and the longitudinal acceleration had very diverse values. For example, in the first segment, the longitudinal acceleration changed quickly from $+4.4\,m\,s^{-2}$ to $-3.6\,m\,s^{-2}$, and the speed grew from zero to around $10\,m\,s^{-1}$: in fact, as long as the longitudinal dynamics did not influence the lateral dynamics, and in particular, the roll angle and its derivatives, it did not affect the segmentation. This consideration extended to all the other signals: for example, Fig. 4b showed that in the last segment, the steering angle δ was slightly negative and not zero, as in the other VR segments. This result was expected, as the last part of the trial had a slight curvature, requiring a small steering rotation. However, as the speed was very low, the roll required was tiny, and the algorithm correctly classified it as a VR segment based on the roll angle and its derivatives. For this reason, the blue cluster was called 'Vertical Riding' and not 'Riding Straight'. This work focused on the lateral dynamics: in case the longitudinal dynamics were also of interest, they could be easily included in the segmentation algorithm by adding the longitudinal acceleration to the input variables, accounting for an appropriate number of additional clusters. K (Number of clusters) could be increased from six to eight to include the 'Vertical Accelerating' and 'Vertical Braking' clusters.

A corner entry manoeuvre is analogous to the first half of a lane change. Cossalter and Sadauckas [10] investigated the latter in-depth, dividing it into different phases through a manual segmentation that considered all the signals measured. He identified three points of interest in the first half of the lane change: the manoeuvre start ('1': $\dot{\phi} \neq 0$, and $\dot{\psi} \neq 0$ towards the outside of the corner); starting to turn towards the corner ('2': $\dot{\psi} = 0$ again); reaching the maximum roll ('3': $\dot{\phi} = 0 \implies \phi = \phi_{max}$). Therefore, the corner entry consisted of two segments: I=1→2 (yawing towards the outside) and II=2→3 (increasing the roll while yawing towards the inside). Despite the fact of using an automatic, unsupervised algorithm and only using the roll angle and its derivatives for the segmentation, this work expanded Cossalter's segmentation. The I segment corresponds to the ALD segment; the II segment equals the concatenation of the LIF and LIE segments. As the LIF and LIE segments have significantly different roll acceleration, steering angle and yaw rate values, they allow describing this corner entry phase with more detail than the single II segment, which lumps together sections with diverse behaviour. Therefore, the manoeuvre that Cossalter divided into two phases was described through three segments, each with a clear physical meaning and statistical characteristics: the method performed a more granular subdivision than the one proposed by a previous article studying the manoeuvre in-depth through manual segmentation.

The proposed unsupervised methodology is based on the TICC algorithm, which simultaneously segments and clusters data according to their correlation. This specificity gives this algorithm many advantages compared to other algorithms based on a methodology where segmentation and clustering are performed separately. The superiority of this algorithm concerning riding-pattern identification emerged clearly in a previous article; therefore, the current work focused on defining suitable signals to describe steady-state and transient lateral dynamics manoeuvres, proposing methodologies for interpreting the clusters obtained (scatterplots and boxplots), and showing the detailed description of motorcycle behaviour in a proposed case-study. First, this algorithm is adapted to consider the temporal characteristics of riding series data. Therefore, this approach could help understand the behaviour in a more fine-grained manner. The second advantage is related to the fact that the algorithm allows a better interpretation of the clusters obtained through the study of the MRF matrix, which is, in the case considered, a great help in explaining the way riders initiate the curve. Interpreting the clusters is required of the user and must be simple and intuitive, as the typical user of such a tool will be an expert in vehicle dynamics, traffic behaviour or a driving instructor, who, in general, will not have knowledge of machine learning.

This work aimed to investigate the proposed segmentation algorithm's results and use them to draw conclusions about in-depth aspects of lateral dynamics. The novelty of the work consisted in adapting the TICC algorithm to the problem of motorcycle lateral (tilting) dynamics and proposing a general approach that leverages graphical representations to quickly interpret the clusters, which are not based on pre-conceived ideas and allow describing the riding task as the concatenation of segments. The methodology is modular, easy to implement, and generalisable to studying the driving behaviour of one or more riders. For conciseness and space constraints, the work used the riding data of a professional riding trainer: this made the riding actions repeatable and sensible. The 'Leaf' shape of the g-g diagram was coherent with this type of experienced rider riding in a controlled environment. A future study should

compare different trials of the same rider, possibly subject to different instructions, and riders with different experience levels. This is a typical application of the algorithm proposed in this work: a researcher has designed and carried out an experiment to verify a certain number of hypotheses; for that purpose, they will segment and use the clusters to verify them. Employing the method in a diverse naturalistic session would make it possible to assess its robustness and validity further.

V. Conclusions and Perspectives

This work proposed an automatic, unsupervised segmentation and clustering tool for riding data. The algorithm identifies and categorises the primitives constituting the various manoeuvres: the generic dynamic of the motion is locally described by the segment to which it belongs. In contrast, the manoeuvre as a whole is defined by the succession of segments. Although the method only requires the measurement of a single signal (the roll angle), it carries out an extensive and detailed description of the lateral dynamics, highlighting secondary behaviour and detecting the start of the manoeuvre very early on. Each cluster is relative to a specific dynamics condition, thus aiding the interpretation of the meaning of each of those conditions.

This method can aid research on human-machine interaction and riding preferences in bends. As the corner entry case study showed, in-depth studies of motorcycle dynamics could also benefit from the resulting segmentation. The approach enables new possibilities concerning the analysis of long, naturalistic sessions, making better use of studies conducted in a more realistic environment. Trainers could use the tool to train and evaluate riders, while insurance experts could employ it to reconstruct the fall dynamics.

Acknowledgment

The authors thank Le Centre national de formationurit routie-Fontainebleau for contributing to the experimentation. They also thank Flavien Delghier for his contribution to the instrumentation.

References

[1] ONISR. (2019). *2018 Road Safety Annual Report*. [Online]. Available: https://www.onisr.securite-routiere.gouv.fr/en/road-safety-performance/annual-road-safety-reports/2018-road-safety-annual-report

[2] WHO. (2018). *Global Status Report on Road Safety 2018*. [Online]. Available: https://www.who.int/violence_injury_prevention/road_safety_status/2018/en/

[3] E. Vlahogianni, G. Yannis, J. C. Golias, N. Eliou, and P. Lemonakis, "Identifying riding profiles parameters from high resolution naturalistic riding data," in *Proc. 3rd Int. Conf. Road Saf. Simulation (RSS)*, Sep. 2011, pp. 14–16.

[4] A. I. Tokey, S. A. Shioma, and S. Jamal, "Analysis of spatiotemporal dynamics of e-scooter usage in Minneapolis: Effects of the built and social environment," *Multimodal Transp.*, vol. 1, no. 4, Dec. 2022, Art. no. 100037, doi: 10.1016/j.multra.2022.100037.

[5] Z. Ma and P. Zhang, "Individual mobility prediction review: Data, problem, method and application," *Multimodal Transp.*, vol. 1, no. 1, 2022, Art. no. 100002, doi: 10.1016/j.multra.2022.100002.

[6] S. Muhle, "An analytical framework for modeling ride pooling efficiency and minimum fleet size," *Multimodal Transp.*, vol. 2, no. 2, Jun. 2023, Art. no. 100080, doi: 10.1016/j.multra.2023.100080.

[7] A. Hula, F. Furnsinn, K. Schwieger, P. Saleh, M. Neumann, and H. Ecker, "Deriving a joint risk estimate from dynamic data collected at motorcycle rides," *Accident Anal. Prevention*, vol. 159, Sep. 2021, Art. no. 106297, doi: 10.1016/j.aap.2021.106297.

[8] M. Diop, A. Boubezoul, L. Oukhellou, and S. Espie, "Powered two-wheeler riding profile clustering for an in-depth study of bend-taking practices," *Sensors*, vol. 20, no. 22, p. 6696, 2020, doi: 10.3390/s20226696.

[9] S. Will et al., "Methodological considerations regarding motorcycle naturalistic riding investigations based on the use of g-g diagrams for rider profile detection," *Saf. Sci.*, vol. 129, Sep. 2020, Art. no. 104840, doi: 10.1016/j.ssci.2020.104840.

[10] V. Cossalter and J. Sadauckas, "Elaboration and quantitative assessment of manoeuvrability for motorcycle lane change," *Vehicle Syst. Dyn.*, vol. 44, no. 12, pp. 903–920, Dec. 2006, doi: 10.1080/00423110600742072.

[11] M. Bartolozzi, G. Savino, and M. Pierini, "Novel high-fidelity tyre model for motorcycles to be characterised by quasi-static manoeuvres—Rationale and numerical validation," *Vehicle Syst. Dyn.*, vol. 60, no. 12, pp. 4290–4316, Dec. 2022, doi: 10.1080/00423114.2021.2013506.

[12] G. Agamennoni, S. Worrall, J. R. Ward, and E. M. Neboty, "Automated extraction of driver behaviour primitives using Bayesian agglomerative sequence segmentation," in *Proc. 17th Int. IEEE Conf. Intell. Transp. Syst. (ITSC)*, Oct. 2014, pp. 1449–1455, doi: 10.1109/ITSC.2014.6957890.

[13] A. Bender, G. Agamennoni, J. R. Ward, S. Worrall, and E. M. Nebot, "An unsupervised approach for inferring driver behavior from naturalistic driving data," *IEEE Trans. Intell. Transp. Syst.*, vol. 16, no. 6, pp. 3325–3336, Dec. 2015, doi: 10.1109/TITS.2015.2449837.

[14] G. Li, Y. Chen, D. Cao, X. Qu, B. Cheng, and K. Li, "Extraction of descriptive driving patterns from driving data using unsupervised algorithms," *Mech. Syst. Signal Process.*, vol. 156, Jul. 2021, Art. no. 107589, doi: 10.1016/j.ymssp.2020.107589.

[15] N. Magiera, H. Janßen, M. Heckmann, and H. Winner, "Rider skill identification by probabilistic segmentation into motorcycle maneuver primitives," in *Proc. IEEE 19th Int. Conf. Intell. Transp. Syst. (ITSC)*, Mar. 2016, pp. 379–386, doi: 10.1109/ITSC.2016.7795583.

[16] M. Diop, A. Boubezoul, L. Oukhellou, S. Espié, and S. Bouaziz, "Powered two-wheelers right-hand curve negotiation study using segmentation and data mining approaches," *IEEE Trans. Intell. Transp. Syst.*, vol. 24, no. 3, pp. 3407–3421, Mar. 2023.

[17] D. Hallac, S. Vare, S. Boyd, and J. Leskovec, "Toeplitz inverse covariance-based clustering of multivariate time series data," in *Proc. 23rd ACM SIGKDD Int. Conf. Knowl. Discovery Data Mining*, Aug. 2017, pp. 215–223, doi: 10.1145/3097983.3098060.

[18] M. Y. Bouaouni, R. A. A. Yahia, and A. Boubezoul, "Driving-pattern identification and event detection based on an unsupervised learning framework: Case of a motorcycle-riding simulator," *IEEE Access*, vol. 9, pp. 158456–158469, 2021, doi: 10.1109/ACCESS.2021.3130400.

[19] M. Bartolozzi, G. Savino, and M. Pierini, "Motorcycle steering torque estimation using a simplified front assembly model: Experimental validation and manoeuvrability implications," *Vehicle Syst. Dyn.*, pp. 1–26, 2023, doi: 10.1080/00423114.2023.2194542.

Mirco Bartolozzi received the master's degree in mechanical engineering from the University of Florence, Florence, Italy, in 2020. He is currently pursuing the joint Ph.D. degree in smart industry from the Universities of Florence, the University of Pisa, and the University of Siena.

He concluded his degree through an internship at Siemens, Leuven, doing an experimental thesis on tyre modeling and parametric identification in driving conditions. From 2018 to 2019, he was a member of the Dynamics and Suspension Assembly of the Formula SAE Team, University of Florence. He was appointed as an assembly chief in 2020 and has been an external supervisor since 2022. His research interests include motorcycle dynamics, tyre behaviour, characterization and modeling, riding simulation, vehicle testing, motorcycle manoeuvrability, rider-vehicle interaction, and riding style.

Abderrahmane Boubezoul received the master's degree in virtual reality and complex systems from Evry Val d'Essone University, France, and the Ph.D. degree in computer science and mathematics from University Paul Canne (Aix-Marseille III), France, in 2008. Since 2008, he has been a Researcher with Gustave Eiffel University. He is conducting his research at the Laboratory of Systems and Applications of Information and Energy Technologies (SATIE Laboratory UMR8029), ENS Paris-Saclay University. His research interests include statistical signal processing and machine learning for road transport systems.

Samir Bouaziz was born in Algeria. He received the Ph.D. degree in electronics from Paris-Sud University (now Paris-Saclay), France, in 1992. He is currently a Full Professor with the Laboratory of Systems and Applications of Information and Energy Technologies (SATIE laboratory UMR8029), ENS Paris-Saclay University. He is also the research team's leader of architecture design of embedded systems for autonomous vehicles. He is also the Director of the Pedagogical IT Department, Paris-Saclay University, the Head of the Department of Electronics Robotics Systems, Engineer School, Polytech Paris-Saclay, and serves on the Governing Council. He is also an Expert for various research funding institutions, such as ANRT, CIR France, and Quebec Research Fund. He is also the Project Leader of the ERASMUS+ Program (2018–2023) with Ecole Nationale Polytechnique Alger and Paris-Saclay University. His research interests include hardware/software (SOC and FPGA) designs of embedded systems for autonomous vehicles and robots. His research is led by time constraints considering the complexity of a good fit between hardware and algorithms. Electronics Instrumentation is one of scientific interest, benchmark systems to understand human-vehicle interactions and hardware-software co-designs.

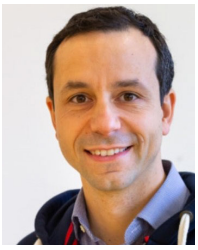

Giovanni Savino is currently an Associate Professor with the University of Florence, Italy, and a Research Associate with the Accident Research Centre, Monash University, Australia. With a background in mechanical engineering, he developed a multidisciplinary expertise in vehicular safety by working on many EC-funded projects to improve motorcyclists' safety, including PISA, Mymosa, Saferider, 2BeSafe, Abram, Motorist, and Pioneers. His research interests include developing and assessing advanced motorcycle safety technologies.

Stéphane Espié is currently a Research Director with Gustave Eiffel University. He is conducting his research in the UMR 8029 SATIE, where he is responsible for the Methods and Tools for Signals and Systems (MOSS) Research Group. His research interests include the design of tools (driving simulators, instrumented vehicles, and behavioural traffic simulation) for studying driver, traffic system behaviours, and vulnerable road users, mainly powered two-wheelers riders.

Open Access funding provided by 'Università degli Studi di Firenze' within the CRUI CARE Agreement